

MIT Open Access Articles

Exciton-phonon coupling in individual GaAs nanowires studied using resonant Raman spectroscopy

The MIT Faculty has made this article openly available. **Please share** how this access benefits you. Your story matters.

Citation: Brewster, Megan et al. "Exciton-phonon coupling in individual GaAs nanowires studied using resonant Raman spectroscopy." *Physical Review B* 80.20 (2009): 201314. © 2009 The American Physical Society

As Published: <http://dx.doi.org/10.1103/PhysRevB.80.201314>

Publisher: American Physical Society

Persistent URL: <http://hdl.handle.net/1721.1/52518>

Version: Final published version: final published article, as it appeared in a journal, conference proceedings, or other formally published context

Terms of Use: Article is made available in accordance with the publisher's policy and may be subject to US copyright law. Please refer to the publisher's site for terms of use.



Exciton-phonon coupling in individual GaAs nanowires studied using resonant Raman spectroscopy

Megan Brewster,¹ Oliver Schimek,² Stephanie Reich,² and Silvija Gradečak^{1,*}

¹*Department of Materials Science and Engineering, Massachusetts Institute of Technology, Cambridge, Massachusetts 02139, USA*

²*Institut für Experimental Physik, Freie Universität, Berlin 14195, Germany*

(Received 19 October 2009; published 25 November 2009)

The Fröhlich coupling strength of individual GaAs nanowires is investigated by resonant micro-Raman spectroscopy measurements near the direct bandgap E_g . Large 2LO/1LO intensities up to 5.7 are observed in an individual GaAs nanowire. A 2LO resonance profile of the GaAs nanowire agrees well with a two-phonon-scattering model, suggesting excitonic scattering. These results advance the understanding of electron-phonon coupling and exciton scattering in quasi-one-dimensional systems and in GaAs at E_g , allowing for the development and optimization of nanowire optoelectronic devices.

DOI: [10.1103/PhysRevB.80.201314](https://doi.org/10.1103/PhysRevB.80.201314)

PACS number(s): 63.22.Gh, 63.20.kd, 71.35.-y, 78.30.Fs

Nanowires are quasi-one-dimensional crystals that can exhibit radial quantum confinement, resulting in nanoscale properties different from those of the bulk. Individual semiconductor nanowires have been employed in nanoscale optoelectronic devices, such as electrically driven lasers,¹ light-emitting diodes,² and photodetectors,³ among other applications.⁴ A fundamental understanding of electron-phonon interaction within nanowires is required to tailor their optical and electrical properties⁵ and could further the development of nanowire electronic devices. For example, photoluminescence peak broadening is largely attributed to the coupling of electronic charge to phonons,⁶ which can inhibit the ability to spectrally distinguish individual photons; further, phonon coupling to the electron of a bound exciton could drastically affect optoelectronic properties in nanowire devices, especially in regimes of strong quantum confinement.^{7,8}

Fröhlich-induced electron-phonon coupling in assemblies of nanowires has been previously investigated under non-resonance conditions.^{9,10} However, a disparity in growth directions, size, and structure of nanowires within an assembly can result in averaged spectral data hindering information on a single-nanowire level. Resonant Raman spectroscopy is sensitive to structural variations of individual nano-objects within a population,¹¹ but no resonant Raman studies on individual nanowires have been reported to date. Here, we study individual nanowires by resonant micro-Raman spectroscopy near the energy bandgap E_g to understand electron-phonon coupling and exciton scattering in quasi-one-dimensional systems. Notably, previous attempts have been hampered by excessive photoluminescence (PL).¹² A model is presented for two-phonon excitonic scattering, which fits well with the observed 2LO resonance intensities from a single GaAs nanowire and allows us to assess the Fröhlich coupling strength and the exciton damping constant.

GaAs nanowires were grown using metalorganic chemical vapor deposition catalyzed by 90 nm Au nanoparticles, as reported previously.¹³ Nanowire structural properties were investigated using a JEOL 6320FV high-resolution scanning electron microscope (SEM) and by JEOL 2010F field-emission transmission electron microscope (TEM). For Raman experiments, nanowires were removed from the growth

substrates by sonication in ethanol and then dispersed onto CaF₂ substrates. Special care was taken to dilute the nanowire solution to achieve single-nanowire measurements. Near-resonance micro-Raman spectroscopy was conducted at room temperature by a fiber-coupled Kaiser HoloLab Series 5000 Raman Microscope with pump laser light of 785 nm and the incident power of 4.0 mW at the sample. The Fröhlich coupling strength of individual GaAs nanowires was investigated at room temperature by resonant micro-Raman spectroscopy through a 100× objective in backscattered configuration with a fully tunable IR laser system over 790–900 nm. Nanowires were excited at the same point for each measurement with a constant incident laser power of 3.6 mW at the sample. To account for the sensitivity of the experimental setup, we normalized the measured Raman spectra to the cross section of a CaF₂ reference crystal with a known Raman cross section. Spectra were calibrated for both Raman shift and intensity prior to peaks fitting assuming Lorentzian-shaped curves and peak intensities were determined by peak area integration.

Prior to characterization by Raman spectroscopy, GaAs nanowires were investigated by electron microscopy to confirm the overall morphology and structural quality of individual nanowires. Figure 1(a) shows an SEM image of GaAs nanowires, as grown on the GaAs (111)B substrate. The uniformity in nanowire lengths, diameters, and shapes, as well as the epitaxial growth of the nanowires from the substrate, indicate strict control over the nanowire growth. A bright-field TEM image of an individual GaAs nanowire [Fig. 1(b)] and corresponding lattice-resolved TEM image [Fig. 1(c)] show that the nanowire is free of dislocations with a length of 7 μm and diameters ranging from 80 to 120 nm, and verifies crystallinity along the length of the nanowire. An accompanying selected-area diffraction pattern in the inset of Fig. 1(c) reveals that nanowires have single-crystal zinc blende structure and grow along the $\langle 1\bar{1}1 \rangle$ direction. These results are consistent among all nanowires investigated in this work. All Raman experiments were performed with the laser spot focused in the same spot near the middle of the nanowire, which we approximate to be 100 ± 5 nm in diameter.

A typical micro-Raman spectrum collected from a single

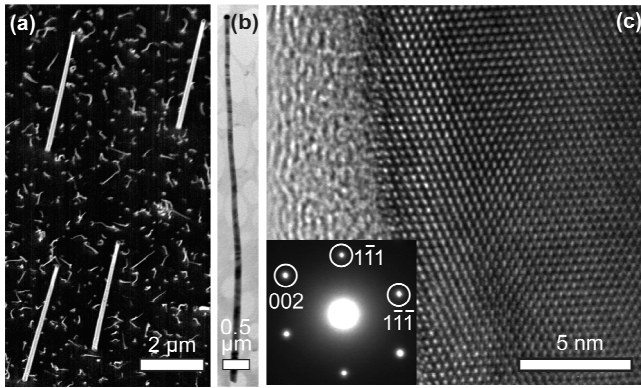


FIG. 1. (a) SEM image of GaAs nanowires as grown on a GaAs substrate. (b) TEM image of a single GaAs nanowire, and (c) corresponding lattice-resolved TEM image and selected-area diffraction pattern along $\langle 110 \rangle$ zone axis (inset), indicating the $\langle 111 \rangle$ growth direction.

GaAs nanowire (excited by 785 nm laser light) shows TO and LO modes at approximately 270 and 293 cm^{-1} , respectively; as well as strong multiphonon modes up to the fourth order (Fig. 2, inset), spaced by one LO phonon frequency. Combinations of the LO and multi-LO modes with the TO mode, 1LO+TO and 2LO+TO, can also be resolved. Interestingly, relative intensities of 1LO and 2LO peaks vary significantly with the incident excitation energy (Fig. 2), indicating the resonance of an electronic transition.

The observation of multiphonon modes is consistent with the Fröhlich coupling between an electron and a macroscopic electric field formed by microscopic deformations of a polar lattice.^{14,15} Strong electric fields can be induced only by the LO modes;¹⁵ since only the LO mode exhibits the cascading phenomenon shown in Fig. 2, this suggests that Fröhlich coupling is the relevant cascade-aiding mechanism in GaAs nanowires. The Fröhlich coupling strength has traditionally been calculated by the Huang-Rhys parameter S .¹⁶ In a simplified model, S is linearly proportional to the ratio of the fundamental to overtone LO Raman intensities (in our case, 2LO/1LO); thus, the Fröhlich coupling strength may be inferred from the relative peak intensities of the cascade Ra-

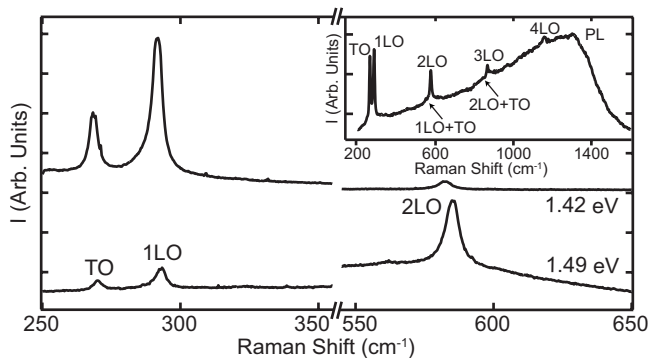


FIG. 2. Truncated micro-Raman spectra of an individual GaAs nanowire at 1LO resonance (1.42 eV, bulk GaAs E_g) and 2LO/1LO resonance (1.49 eV, $E_g + 2\hbar\omega_{LO}$). Inset shows a full multiphonon spectrum away from resonance. First order, higher order, and combination Raman modes, as well as a broad PL peak, are indicated.

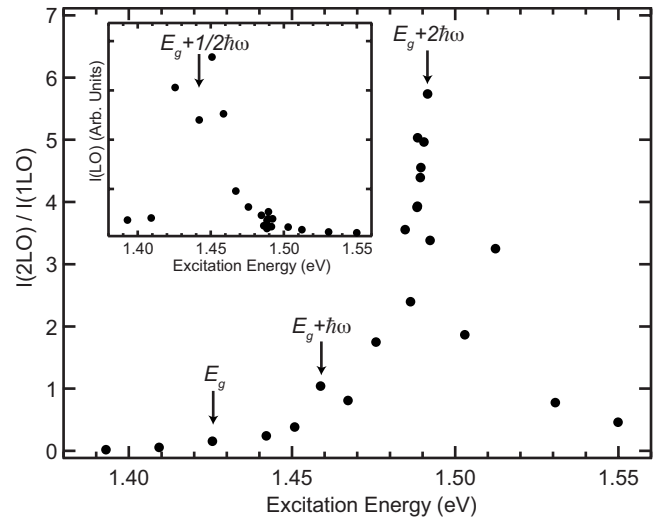


FIG. 3. Resonance profile of 2LO/1LO intensity ratios for an individual GaAs nanowire, with sharp resonance at two phonon energies above the direct bandgap ($E_g + 2\hbar\omega_{LO}$). Inset shows 1LO intensity, with a broad maximum around $E_g + \frac{1}{2}\hbar\omega_{LO}$. Error in the data due to the curve fitting is less than 3%.

man spectrum.^{5,16,17} The resonance profile of an individual GaAs nanowire in Fig. 3 shows a sharp outgoing resonance at 5 meV below $E_g + 2\hbar\omega_{LO}$ with 2LO/1LO ratios as high as 5.7, a small shoulder at 2 meV below $E_g + \hbar\omega_{LO}$, and no incoming resonance feature at E_g . Here, the blueshift of the bulk E_g value¹⁸ due to quantum confinement in nanowires with 100 nm diameters was estimated to be 0.5 meV, while the GaAs LO phonon energy $\hbar\omega_{LO} = 0.03614$ eV was calculated as the average of all measured LO mode frequencies. The resonance profile of the 1LO mode of the same individual GaAs nanowire is shown in the inset of Fig. 3, with a broad maximum around $E_g + \frac{1}{2}\hbar\omega_{LO}$, consistent with intrinsic Raman scattering.¹⁴ However, the distribution of the measured data points suggests that further experimentation is necessary to confirm intrinsic scattering instead of impurity scattering, which is characterized by an asymmetric maximum around $E_g + \hbar\omega_{LO}$.

Comparing Fröhlich coupling strength in GaAs nanowires with bulk values can be challenging because it is a theoretical value that depends only upon the LO phonon frequency and the dielectric constant.¹⁴ The closely related S parameter can be employed only with a detailed analysis of the resonance conditions, vibrational modes, and excitonic states in the ensemble.¹⁹ In addition, excessive PL at the direct bandgap transition has hampered all previous attempts in bulk GaAs,¹² which makes comparison of the Fröhlich coupling strength in the GaAs nanowire system to that in the bulk at $E_g + 2\hbar\omega_{LO}$ impossible. Relatively low PL signal in nanowires in comparison to the bulk may be due to PL quenching by the multitude of charged states on the nanowire surface, such as V_{As} , allowing for enhanced resolution of the Raman modes. The closest comparison that can be made is with the work of Trommer and Cardona, who reported a maximum 2LO/1LO ratio of 0.25 at $E_g + \Delta_0 + 2\hbar\omega_{LO}$ for (110) bulk GaAs, where Δ_0 is the split-off orbital energy;²⁰ our maximum 2LO/1LO ratio of 5.7 at $E_g + 2\hbar\omega_{LO}$ implies that

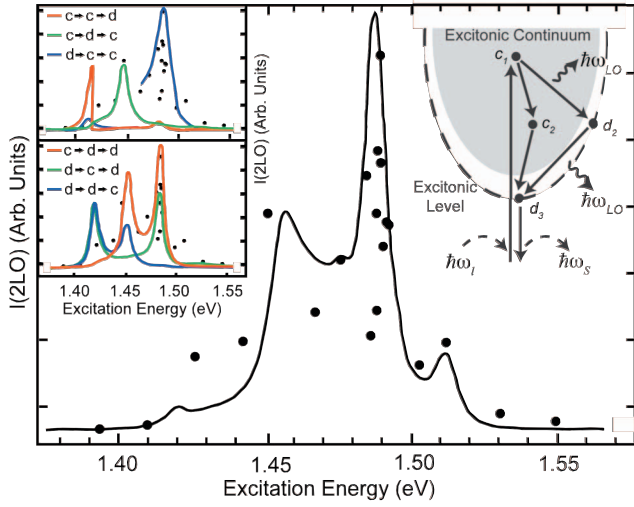


FIG. 4. (Color) 2LO resonance profile from a single GaAs nanowire. Dots are experimental data, solid lines represents the calculated model. Unweighted individual sequences are shown in the left inset. Schematic of two-phonon excitonic scattering in an excitonic band scheme is shown in the inset on the right, with two scattering sequences, $c \rightarrow c \rightarrow d$ and $c \rightarrow d \rightarrow c$ presented, after Ref. 21. Incident excitation energy $\hbar\omega_i$ creates a continuous (unbound) exciton, which scatters successively to either c or d (bound) states, emitting a phonon of energy $\hbar\omega_{LO}$ with each transition. The exciton finally recombines at the base of the excitonic level, emitting a scattered photon with energy $\hbar\omega_s$.

Fröhlich coupling in GaAs nanowires is significantly stronger than that for bulk GaAs at a nearby transition.

LO cascade action with periodicity of $\hbar\omega_{LO}$ implies excitonic transitions because the relaxation of an unbound exciton to a bound state is mediated by phonons.^{21,22} While the single-phonon cascade model²² can explain existence of multiphonon modes, it does not account for our observation of $2LO/1LO > 1$ at resonance.⁸ On the other hand, a two-phonon excitonic scattering model by García-Cristóbal²¹ correlates well with our results. We present here a simplified version of this model to verify two-phonon excitonic transitions in a single GaAs nanowire under resonant conditions.

When a photon impinges on a crystal, a virtual exciton in the internal state α is formed; the exciton is then relaxed through a two-step process via intermediate states β and γ , forming an LO phonon of frequency ω_{LO} at each step (Fig. 4, inset). Excitonic intermediate states can be either continuous unbound excitonic state (c), or discrete bound excitonic state (d), so a two-step excitonic transition can be represented by eight permutations of three consecutive intermediate states of these two types. Each of the intermediate states can be characterized by the exciton center-of-mass wave vector (\mathbf{K}) and the internal exciton wave vector (\mathbf{k}), but for the initial and the final states $\mathbf{K} = 0$ because the incoming and outgoing photons have negligible wave vectors and momentum is conserved throughout the process. The quantum-mechanical scattering amplitude $W_{\alpha\beta\gamma}$ for each scattering process can be described as follows:

$$W_{\alpha\beta\gamma} \propto \int_0^\infty dk \frac{1}{(\hbar\omega_l - E_\alpha + i\Gamma_\alpha)} \times \frac{1}{(\hbar\omega_l - \hbar\omega_{LO} - E_\beta + i\Gamma_\beta)} \times \frac{1}{(\hbar\omega_l - 2\hbar\omega_{LO} - E_\gamma + i\Gamma_\gamma)}, \quad (1)$$

where $\hbar\omega_l$ is the energy of the incident laser light, $E_{\alpha,\beta,\gamma}$ and $\Gamma_{\alpha,\beta,\gamma}$ are energy and the width (i.e., damping constant), respectively, of the corresponding excitonic state. We assume constant matrix elements for electron-photon and electron-phonon couplings, as these have negligible effect on the shape of the profile¹⁴ and are inconsequential to the final intensity of the resonance profile, as the calculated model intensity is scaled manually to match that observed experimentally. The energy of the excitonic states can be described as

$$E_d = E_g + \frac{\hbar^2 K^2}{2m_e} - \frac{\mathcal{R}}{n^2} \quad (2)$$

$$E_c = E_g + \frac{\hbar^2 K^2}{2m_e} + \frac{\hbar^2 k^2}{2\mu} \quad (3)$$

for a discrete and continuous state, respectively. Here, E_g is the energy band gap (for GaAs nanowires, $E_g = 1.423$ eV is calculated from the fit), \mathcal{R} is the Rydberg constant, $n = 1, 2, \dots$ is the principle quantum number of the hydrogen-like bound state, and $\mu = m_e m_h / (m_e + m_h)$ is the reduced mass calculated from the effective electron (hole) mass in GaAs $m_e = 0.063m_E$ ($m_h = 0.51m_E$), with m_E the rest mass of an electron.¹⁸ Finally, the 2LO Raman scattering intensity can be calculated by integrating the square of the sum of all of the scattering amplitudes over all \mathbf{K} wave vectors,

$$I_{2LO} = \int_0^\infty dK \left| \sum_{\alpha,\beta,\gamma} W_{\alpha\beta\gamma} \right|^2. \quad (4)$$

First, we have calculated separately 2LO Raman scattering contributions for each of eight scattering pathways (Fig. 4, inset), assuming that the lowest exciton state ($n=1$) is the only level that provides significant contribution to the shape of the Raman intensity profile. From these calculations, we find the most important contributions to the scattering intensity are $c \rightarrow c \rightarrow d$, $c \rightarrow d \rightarrow c$, $d \rightarrow c \rightarrow c$, $c \rightarrow d \rightarrow d$, $d \rightarrow c \rightarrow d$, and $d \rightarrow d \rightarrow c$; while $c \rightarrow c \rightarrow c$ and $d \rightarrow d \rightarrow d$ have negligible contributions and were excluded from further calculations. Each of these six contributions were manually weighted prior to integration over \mathbf{K} . We found the excitonic damping constants Γ_c (Γ_d) for continuous (discrete) states to be 9 meV (5 meV), regardless of the exciton wave vectors \mathbf{K} and \mathbf{k} .

The model fits well with the 2LO data of the GaAs nanowire (Fig. 4), confirming two-phonon excitonic transitions are responsible for the scattering processes in a GaAs nanowire, similar to the predictions for the bulk. However, the damping parameter $\Gamma_d = 5$ meV is smaller than the damping of 7 meV reported for the bulk at $E_g + \Delta_0$.²¹ A smaller damping factor in nanowires at the E_g transition, as compared to the bulk at $E_g + \Delta_0$, implies stronger exciton-phonon coupling and confinement of the exciton wave function.⁵ Further en-

hancement of exciton-phonon coupling in comparison to the bulk is likely due to strong coupling to charged surface states,²³ as the surface-to-volume ratio is larger in one-dimensional nanowires than in the three-dimensional bulk.

In conclusion, significant Fröhlich coupling, stronger than in any materials systems of any dimensionality published to date, is observed in an individual GaAs nanowire. We verify two-phonon excitonic scattering by modeling, and find that the excitonic damping parameters are smaller than those reported in the bulk at $E_g + \Delta_0$. We contribute the Fröhlich coupling enhancement in GaAs nanowires over the bulk to exciton-phonon interactions, smaller damping parameters, and coupling of excitons to charged surface states. GaAs nanowire devices, such as excitonic transistors,²⁴ whose performance is dependent on prolonged polarization or narrow

excitonic transition linewidths will benefit from these smaller damping factors. To further understand the effects of Fröhlich coupling on excitonic scattering, future investigations will focus on the effects of nanowire diameter on coupling strength, especially below the exciton Bohr diameter limit.

We thank S. K. Lim and E. Nanni for technical assistance. This work made use of the Shared Experimental Facilities supported in part by the MRSEC Program of the National Science Foundation under Award No. DMR-0819762. M.B. acknowledges funding from NSF, DOD, and MISTI Germany. This work was supported in part by NSF CAREER Award No. DMR-0745555 (S.G.) and by ERC Project No. 210642-OptNano (S.R.).

*gradecak@mit.edu; <http://web.mit.edu/gradecakgroup/index.html>

- ¹X. Duan, Y. Huang, R. Agarwal, and C. M. Lieber, *Nature (London)* **421**, 241 (2003).
- ²F. Qian, Y. Li, S. Gradecak, D. Wang, C. J. Barrelet, and C. M. Lieber, *Nano Lett.* **4**, 1975 (2004).
- ³J. Wang, M. S. Gudiksen, X. Duan, Y. Cui, and C. M. Lieber, *Science* **293**, 1455 (2001).
- ⁴R. Agarwal and C. M. Lieber, *Appl. Phys. A: Mater. Sci. Process.* **85**, 209 (2006).
- ⁵X. B. Zhang, T. Taliercio, S. Kolliakos, and P. Lefebvre, *J. Phys.: Condens. Matter* **13**, 7053 (2001).
- ⁶P. Bhattacharya, *Semiconductor Optoelectronic Devices* (Prentice Hall, Upper Saddle River, NJ, 1997).
- ⁷G. D. Scholes and G. Rumbles, *Nature Mater.* **5**, 683 (2006).
- ⁸*Semiconductor Nanocrystal Quantum Dots*, edited by A. L. Rogach (Springer Wien, New York, 2008).
- ⁹R. P. Wang, G. Xu, and P. Jin, *Phys. Rev. B* **69**, 113303 (2004).
- ¹⁰S. Dhara *et al.*, *Appl. Phys. Lett.* **90**, 213104 (2007).
- ¹¹F. Wang, W. Liu, Y. Wu, M. Y. Sfeir, L. Huang, J. Hone, S. O'Brien, L. E. Brus, T. F. Heinz, and Y. R. Shen, *Phys. Rev. Lett.* **98**, 047402 (2007).
- ¹²A. K. Sood, W. Kauschke, J. Menéndez, and M. Cardona, *Phys.*

Rev. B **35**, 2886 (1987).

- ¹³M. J. Tambe, S. K. Lim, M. J. Smith, L. F. Allard, and S. Gradecak, *Appl. Phys. Lett.* **93**, 151917 (2008).
- ¹⁴P. Y. Yu and M. Cardona, *Fundamentals of Semiconductors: Physics and Materials Properties*, 3rd ed. (Springer, Berlin, 2005).
- ¹⁵G. D. Mahan, *Many Particle Physics* (Kluwer Academic/Plenum Publishers, New York, 2000).
- ¹⁶K. Huang and A. Rhys, *Proc. R. Soc. London, Ser. A* **204**, 406 (1950).
- ¹⁷I. Brener, M. Olszakier, E. Cohen, E. Ehrenfreund, A. Ron, and L. Pfeiffer, *Phys. Rev. B* **46**, 7927 (1992).
- ¹⁸S. Adachi, *J. Appl. Phys.* **58**, R1 (1985).
- ¹⁹R. Rodríguez-Suárez, E. Menéndez-Proupin, C. Trallero-Giner, and M. Cardona, *Phys. Rev. B* **62**, 11006 (2000).
- ²⁰R. Trommer and M. Cardona, *Phys. Rev. B* **17**, 1865 (1978).
- ²¹A. García-Cristóbal, A. Cantarero, C. Trallero-Giner, and M. Cardona, *Phys. Rev. B* **49**, 13430 (1994).
- ²²R. Martin and C. Varma, *Phys. Rev. Lett.* **26**, 1241 (1971).
- ²³T. D. Krauss and F. W. Wise, *Phys. Rev. B* **55**, 9860 (1997).
- ²⁴G. Grosso, J. Graves, A. T. Hammack, A. A. High, L. V. Butov, M. Hanson, and A. C. Gossard, *Nat. Photonics* **3**, 577 (2009).